Talens Vila, C.; Castro Giraldez, M.; Fito Suñer, PJ. (2018). Effect of Microwave Power Coupled with Hot Air Drying on Sorption Isotherms and Microstructure of Orange Pee. Food and Bioprocess Technology. 11(4):723-734. doi:10.1007/s11947-017-2041-x

Effect of microwave power coupled with hot air drying on sorption isotherms and microstructure of orange peel

Clara Talens[a], Marta Castro-Giraldez[b*], Pedro J. Fito[b]

[a]*AZTI - Food Research, Parque Tecnológico de Bizkaia, Astondo Bidea, Edificio 609, 48160, Derio (Bizkaia), Spain*

[b]*Instituto Universitario de Ingeniería de Alimentos para el Desarrollo, Universitat Politècnica de València, Camino de Vera s/n, 46022 Valencia, Spain*

*author for correspondence: marcasgi@upv.es

ABSTRACT

Drying is one of the most cost-effective methods of worthwhile by-product valorisation. This study had two main objectives. The first was to determine the effect of hot air drying (HAD) combined with microwave (MW) irradiation on the treatment kinetics and the macrostructural and microstructural properties of the dried product. The second aim was to develop engineering tools to predict the extent of dehydration. Drying was performed using hot air at 55 ºC and the combined (HAD + MW) treatment at different power intensities (2 W/g, 4 W/g and 6 W/g). After 5, 15, 40, 60 and 120 min, the mass, surface, volume, water activity and moisture were measured in fresh and dried samples. Sorption isotherms were obtained and fitted to the GAB model, with high correlation coefficients. The macroscopic and microscopic analyses showed shrinkage and swelling in the peel tissue caused by the MW treatment. The HAD + MW methods not only resulted in increased moisture reduction but also induced microstructural changes that generated higher sorption capacity.

Keywords: hot air–microwave drying, orange peel, isotherm, isosteric heat, microstructure, water retention capacity

1. INTRODUCTION

The current environmental problems, especially the global warming effects, call for an increased efficiency in all production systems. Since one of the most efficient ways of decreasing the environmental impact of food production is to obtain more products from the available raw materials, upgrading food by-products is becoming an increasingly important issue (Waldron 2009). The high-value-added products obtained from vegetable by-products are mainly fibres and antioxidant compounds. In recent years, considerable changes in eating habits have been observed in many societies, mainly driven by the desire to lead a healthy lifestyle. These changes have been reflected in an increased consumption of medically recommended foods, resulting in the expansion of the dietary fibre market and the creation of new products with high fibre content (Gómez et al. 2015). Juice industry by-products are very susceptible to microbial spoilage, fermentation or chemical deterioration due to the resident microflora and the endogenous enzymatic activities. Therefore, the methods improving the quality of by-products to be used as value-added food ingredients must include treatments minimising the negative effect of these biological or chemical processes. The most important among such treatments are the dehydration methods reducing the water activity, directly affecting the contaminant microflora (Fava et al. 2013; Fernández-López et al. 2009; Larrauri 1999; Schieber et al. 2001).

The theoretical mechanisms of HAD treatments are based on water fluxes from the food sample to the air stream, induced by a water chemical potential (Demirel and Sandler 2001). The main driver of water transport is the gradient between water activity (a_w) and relative humidity (Traffano-Schiffo et al. 2014). During HAD (below 100 ºC), water evaporation occurs on the product surface. In such cases, it is useful to couple the HAD

with other techniques to increase removal of the water. MW irradiation is the technique commonly combined with HAD (Bergese 2006; Kowalski et al. 2005).

In Europe, the magnetrons used to generate microwaves work at 2.45 GHz. At this frequency, the interactions of the photon flux with biological tissue produce γ-dispersion (orientation polarisation of the water molecules). This dispersion is due to the orientation and induction of dipolar molecules, resulting in the storage of electric energy and its dissipation into other energies such as heat. The main dipolar molecule in orange peel tissue is water (Castro-Giráldez et al. 2010; Castro-Giráldez et al. 2011a; Castro-Giráldez et al. 2011b); therefore, MW heating is directly associated with the quantity and mobility of the water molecules.

The relationship between food moisture and the a_w level is described by the moisture sorption isotherm. Moisture sorption isotherms are important in shelf-life predictions due to their sensitivity to moisture changes. Various mathematical models have been developed to express the relationship between the a_w of the food and its moisture content (Labuza 2007). Guggenheim, Anderson and de Boer developed their GAB model as an improved version of the BET model for multilayer adsorption (van den Berg and Bruin 1981). The GAB equation effectively represents the experimental data in the a_w range from 0 to 0.95 for most foods, such as corn flour, passion fruit peel, pineapple peel, dried tomato pulp, pear, banana pulp, mango pulp, walnut kernels, etc. (Andrade et al. 2011). The model uses three constants. Two of these were obtained from the BET representation, the monomolecular moisture layer X_{w0} and the energy constant C related to the isosteric heat of sorption (Q_c). The parameter C represents the binding strength of water molecules to the primary binding sites on the sample surface (monolayer). The higher the values of C, the stronger are the bonds between water molecules in the monolayer and the binding sites on the surface of the sorbent. The third constant in the GAB model is an empirical

parameter, K. This parameter is a correction factor for multilayer molecules, relative to the liquid phase (Quirijns et al. 2005). This physical meaning, the GAB equation predicts the moisture sorption isotherms of food products over a wide range of a_w. It can also describe some of the temperature effects on the isotherms. Thus, it is the preferred model to fit the moisture sorption behaviour of dried orange products (Edrisi Sormoli and Langrish 2015).

Further analysis of sorption isotherm data by application of thermodynamic principles can provide important information on the energy requirements of dehydration process, food microstructure, physical phenomena on the food surfaces, water properties and sorption kinetics parameters (Rizvi and Benado 1984). Thermodynamic functions adopted for analysis of sorption phenomena include differential enthalpy and entropy and integral enthalpy and entropy. The isosteric heat of sorption, or differential enthalpy of sorption, gives a measure of the water–solid binding strength (sorption energy). Obtaining the isosteric heat is of great importance in the design of equipment for dehydration processes. The heat of vapourisation of adsorbed water might become greater than the heat of vapourisation of pure water as the food is dehydrated to low moisture levels. The isosteric heat greater than the heat of vapourisation indicates that the energy of interactions between the water molecules and sorption sites is greater than the energy that holds the water molecules together in the liquid state. Consequently, the level of moisture at which the isosteric heat approaches the heat of vapourisation of pure water is often indicative of the amount of bound water in the food (Al-Muhtaseb et al. 2002).

A study of Fava et al. (2013) has reported that MW drying of citrus peel results in a stabilised product. This product can be further converted into the dietary fibre with optimal microbial, sensory and technological properties (such as water retention capacity, WRC). During HAD, high temperatures or long drying periods may seriously damage the

product flavour, colour and nutrients, resulting in shrinkage and a decrease in the WRC. MW absorption provokes the internal water heating and evaporation, greatly increasing the internal pressure and concentration gradients and, thus, the effective water diffusion. Consequently, the processing time is reduced, resulting in an improved product quality (Igual et al. 2010). It is quite common to combine the HAD and the MW system. The hot air is, by itself, relatively efficient at removing free water at or near the surface, whereas the unique pumping action of microwave energy helps to remove the internal free water (Schiffmann 2001). An appropriate combination of the two methods may improve the efficiency and the economics of the drying process. Talens et al. (2016a) have developed a thermodynamic model for hot air microwave drying of citrus peel; it explains the mechanisms involved in mass and energy transport throughout the drying process in this combined system. The authors have shown that, depending on the predominant mechanism (shrinkage during HAD or swelling during microwaving), the samples can undergo volumetric expansion or contraction. Ghanem et al. (2012) have studied the MW drying characteristics of *Thompson Navel* oranges (at power levels ranging from 5 to 30 W/g) and the effect of MW treatment on the shrinkage and WRC. Their results show that drying at low MW power (5–15 W/g) gives the maximum WRC. Bejar et al. (2011) have demonstrated that the water-holding capacity increases with the increasing MW power.

By examining the sorption isotherms of orange peel dried using different methods, the efficiency of the processes needed to stabilise this by-product might be improved. This should facilitate the further recovery to utilise it as a value-added food ingredient such as dietary fibre. Moreover, the analysis of microstructural changes occurring during drying might help to predict the functionality of such ingredients.

Therefore, the aim of this work was to determine the sorption isotherms and the isosteric heat of sorption of orange peel submitted to combined hot air and microwave drying and to study its effect on the macrostructure and microstructure of the material.

2. MATERIALS AND METHODS

Oranges (*Citrus sinensis* (L.) Osbeck *var* Washington Navel) were bought from a local supermarket in Valencia (Spain), and their peel was used for the experiments. Sixty orange peel cylinders (20-mm diameter and 3-mm thickness) were obtained using a core borer.

The size and shape of the samples were designed to resemble the small pieces of orange peel left after mechanical extraction of juice and the cuts made by a hammer crusher machine in the processing of orange peel. A diagram of the experimental procedure is shown in Figure 1.

Samples were subjected to HAD and microwave-assisted air drying (HAD + MW, Figure 2), using a specially designed MW-air drying oven (Martín 2003) with a maximum output of 2000 W at 2450 MHz. The oven was connected to a computer to register the temperature of ambient air and hot air, relative humidity of the ambient air and the incident microwave energy. To measure the incident and reflected energy, a directional coupler with power meter was also installed in the waveguide of the magnetron and connected to the computer. The microwave energy transformed to heat energy was quantified following the model of Talens et al., 2016a. Two tubes (diameter of 105 mm) were connected to the modified microwave, one to deliver hot air and the other for the generation and application of the microwaves. The drying compartment had a Teflon chamber (edge = 100 mm) and a mode stirrer to ensure a homogeneous distribution of microwaves. For process control in the drying chamber, several variables were measured. The air temperature was examined using a Pt100 thermocouple and air velocity, using a

148 fan anemometer (inside the Teflon chamber, before the experiment; TESTO 425
149 anemometer, precision ± 0.03 m/s).

150 For the experiments, the air velocity was 2.5 m/s, hot air temperature was 55 ºC, and the
151 MW emitted energy by time or emitted power (E_{MW}) was 0, 2, 4 or 6 W/g. The MW
152 power (W/g) refers to the initial mass of the sample. The microwave energy applied
153 (determined using the IEC-test) was adjusted to avoid burning during the drying process.

154 To facilitate the mass transfer, the orange peel samples were placed on the dryer grid with
155 the flavedo side up. Four drying experiments were carried out (HAD, HAD + 2 W/g,
156 HAD + 4 W/g and HAD + 6 W/g). Three orange peels samples (triplicate) were used for
157 each drying time (5, 15, 40, 60 and 120 min) in each drying experiment. After the drying,
158 the samples were equilibrated at 25 ºC for 1 h in disposable AquaLab® sample cups
159 sealed with Parafilm®, in order to eliminate the concentration profiles in samples.

160 Samples were weighed using a precision balance Mettler Toledo AB304-S (precision: ±
161 0.001 g). Surface water activity was determined employing a dew point hygrometer
162 Decagon Aqualab®, series 3 TE (precision: ± 0.003, dimensionless) (Decagon Devices
163 Inc., Pullman, WA, USA). Measurements were performed using structured (not minced)
164 samples; thus, the obtained a_w was considered the surface a_w. The water content of
165 representative fresh orange peel sample and the samples dried for 120 min was
166 determined. The samples were dried in a vacuum oven at 60 ºC until constant weight was
167 reached (AOAC method 934.06 2000). The moisture content of the samples at the
168 intermediate stages was calculated from the weight loss during drying. Volume was
169 determined by image analysis (Sony T90, Carl Zeiss optics), using Adobe Photoshop©
170 software, obtaining the diameter and thickness of the samples in triplicate.

171 The microstructure of fresh and dried samples was analysed using Cryo-SEM. A
172 CryoACryostage CT-1500C unit (Oxford Instruments, Witney, UK), coupled to a Jeol
173 JSM-5410 scanning electron microscope (Jeol, Tokyo, Japan), was employed. The
174 sample was immersed in slush N_2 (-210 ºC) and then quickly transferred to the cryostage
175 (at 1 kPa) where sample fracture took place. The sublimation (etching) was carried out at
176 -95 ºC. The final point was determined by direct observation under the microscope (at 5
177 kV). Then, the sample was coated with gold under vacuum (0.2 kPa) for 3 min, with
178 ionisation current of 2 mA. The scanning electron microscope observations were carried
179 out at 15 kV, at the working distance of 15 mm and the temperature ≤ -130 ºC.

180 The samples were also examined under a Leica MZ APO™ stereomicroscope (Leica
181 Microsystems, Wetzlar, Germany) with a magnification of 8× to 80×, using the incident
182 light illumination (light reflected off the surface of the sample).

183 The desorption isotherms were obtained using dynamic desorption method of Traffano-
184 Schiffo et al. (2015) and fitted to the GAB model using Equation 1 (van den Berg and
185 Bruin 1981):

186 $$X_W = \frac{X_{W0}\, C\, a_w}{(1-K\, a_w)(1+(C-1)a_w)} \quad (1)$$

187 where X_w corresponds to the average moisture (kg_w/kg_{dm}) of orange peel, X_{W0} is the
188 monomolecular moisture layer (kg_w/kg_{dm}), C is the energy constant and K, the empirical
189 parameter (both dimensionless (Labuza 2007)) and a_w is the surface water activity.
190 For the determination of WRC, approximately 0.5 g of each sample (precision ± 0.0001
191 g) was hydrated in 20 mL of distilled water in a 50 mL Falcon tube and left overnight to
192 ensure that full hydration of the fibre. Then, the tubes were centrifuged at 1000 × g for 10
193 min (adapted from Robertson et al. 2000). The supernatant was decanted, and the tubes
194 were carefully inverted to drain the residual unbound water. The remaining pellet was

dried until constant weight in an oven at 100 ± 5 ºC and weighed to examine the solid matter losses during the draining step. The WRC was calculated as the amount of water retained by the pellet (kg_w/ kg_{dm}).

To determine the statistical significance of the results, an analysis of variance (ANOVA) was carried out with confidence levels of 95 % ($p \leq 0.05$) and 99 % ($p \leq 0.01$) using the Statgraphics Plus 5.1 programme.

3. Results and discussion

Figure 3 shows the changes in the moisture content throughout the time during the different drying treatments. At the initial stages of drying, the samples undergoing HAD + MW treatment lost the moisture faster than those submitted to HAD. Microwave radiation induces the alignment of water molecules, storing some of the energy and dissipating a part of it as thermal energy. In the samples with a large number of water molecules, more thermal energy is produced than in materials with low moisture content. Thus, the main effect of microwave irradiation is observed at the beginning of the drying process. The thermal and mechanical energy levels are increased by microwaving, improving the water molecule motion (increasing the free energy in the media). The process boosts the levels of thermal energy available for water evaporation, reducing the air internal energy losses. During the drying process, the absorbed MW energy decreases with the decreasing water content (Talens et al., 2016a). The interactions between water molecules and microwaves increase with the increasing MW power; however, it will be diminished in samples with reduced water content. These interactions are illustrated in Figure 3; after 5 min, only the maximum MW power, 6 W/g, produced strongly significant effect ($p \leq 0.01$) in comparison with the remaining treatments. After 15 min, significant differences between the moisture content ($p \leq 0.01$) were observed between samples treated with 4 W/g and 6 W/g microwaves and the others. After 40 min, strongly

significant differences ($p \leq 0.01$) were seen between the samples undergoing the HAD and 2 W/g drying procedures and the rest of the samples. After 60 min, no differences were observed because the low moisture content of samples reduced the effect of the MW energy. Also, after 60 min of drying, the results of the treatments converged to the threshold of the thermodynamic properties of dry air ($a_w|^{sample} \approx \varphi|^{air}$).

To understand the structural changes caused by the MW treatment during the HAD, a surface desorption isotherm for each treatment was obtained (Figure 4). The surface desorption isotherms fitted well the GAB model adapted for dynamic measurements (Traffano-Schiffo et al., 2015), with the correlation coefficients of 0.9342, 0.9182, 0.9197 and 0.8493 for HAD, HAD + 2 W/g, HAD + 4 W/g and HAD + 6 W/g, respectively. Sorption isotherms were sorted by MW power. In Figure 4, for the same moisture value the samples with MW and HAD show lower values of water activity because the application of MW energy increases the drying kinetics.

GAB model uses three constants, the monomolecular moisture layer (X_{W0}), the energy constant C (related to the Q_c, the isosteric heat of sorption) with the physical meaning and an empirical constant K. The value of the empirical constant K was 0.981 ± 0.006 for all drying treatments; this constant produces exponentially shaped isotherm to fit the data of samples with liquid phase. This value was the same for all treatments because it depends on the nature of the liquid-phase compounds; the composition of raw material was identical in all cases. However, the GAB parameters with physical meaning were different for each treatment; they were useful in the determination of the effect of microwave energy on the final physical properties of dried product (Figure 5). As X_{W0} represents the monomolecular moisture layer, the application of increased MW levels produced an increase of the isosteric heat or adsorption energy of the monomolecular layer, improving the surface tension of samples and thus the hygroscopicity (Talens et al., 2016b). The

value of the energy constant, C, also increased with the MW power. This parameter is related to the isosteric heat of sorption and, therefore, to the surface tension, the ability of the tissue to store adsorbed water.

The isosteric heat can be calculated using the punctual estimation of the parameter C and the surface temperature of samples, as described in the study of Talens et al. (2016b), following Equation 2 (Labuza 2007).

$$Q_c = RT \ln C \qquad (2)$$

where Q_c is the isosteric heat of sorption (kJ/mol), R is the ideal gas constant (J/mol K) and T is the absolute temperature (K).

Figure 6 shows the relationship between the isosteric heat of sorption and the moisture content of samples. The results (from 1 to 10 kJ/mol) were within the range reported by other authors: 0 to 9 kJ/mol for spray-dried orange juice using isotherms at 20– 50 ºC (Edrisi Sormoli and Langrish 2015), 1.8 to 8 kJ/mol for orange peel with isotherms at 40–60 ºC (Bejar et al. 2011), 0.8 to 8 kJ/mol for dried banana with isotherms at 10– 40 ºC (Yan et al. 2008) and 5 to 30 kJ/mol for pineapple with isotherms at 20–50 ºC (Hossain et al. 2001).

Treatments using high microwave power resulted in a fast reduction in the isosteric heat at the beginning of drying. However, its values, after reaching the minimum, grew increasingly fast during the remaining period, to reach the highest values at the end of treatment. This occurred because, at drying temperature of 55 ºC, the evaporation caused by chemical potential gradients of the water occurs on the surface, moving the water in a liquid state through the sample. However, the MW treatment produces internal evaporation (caused by the penetration depth of radiation), resulting in the internal vapour fluxes and water expansion. This enlarges the pores inside the samples and the internal surface area. Figure 6 shows that, at the end of drying, isosteric heat increases with MW

power, raising the hygroscopicity of the samples. However, the surface tension (σ) represents the free energy available to join the water molecules to the solid structure represented by the surface area (dG/dA). Therefore, if the isosteric heat and the internal surface area increase with the MW power, then the surface tension will also increase.

Talens et al. (2016a) have developed a thermodynamic model to explain and quantify the effect of microwaves and hot air in drying treatments. The authors analysed the coupled mechanisms removing the water and producing swelling, depending on the air properties (temperature, relative humidity, etc.), the surface water activity of the sample and the penetration depth of microwave energy. The shrinkage/swelling effect induced by the penetration depth of the microwave energy can affect the internal water/tissue properties. Figure 7 shows the volume variation for the samples undergoing different drying treatments.

The samples dried by HAD demonstrated a continuous shrinkage associated with the water loss. In such samples, the internal water is transported in a liquid state to the surface where it evaporates, driven by the water chemical potential gradient. After 60 min of drying, the samples reach volume equilibrium associated with the convergence with the thermodynamic properties of dry air ($a_w|^{sample} \approx \varphi|^{air}$). In contrast, the volumes of samples dried using HAD + MW varied throughout the experiment. At the beginning of the treatment, a drastic reduction in the volume was observed, associated with the evaporation of water from the surface. As mentioned above, at some point, the microwave irradiation triggers the internal evaporation of water, coupled with the loss of surface water. These internal vapour fluxes and water expansion cause the swelling (volumetric expansion). At the end of the drying treatment (after 60 min), the volume equilibrium was reached due to the combined effect of the vitreous transition (the glass transition moisture was reached) and the small amount of water remaining in the samples (see Figure 3).

295 The WRC is the most common parameter used to characterise the rehydration capacity of
296 the fibre. However, it is difficult to increase the WRC as it is associated with several
297 mechanisms of water immobilisation (mechanical or electrical behaviour). Therefore, the
298 different mechanisms associated with WRC should be considered in strategies designed
299 to improve the fibre properties related to water interactions.

300 The aim of this study was to develop engineering tools to produce the fibre for human
301 consumption from the by-products of citrus juice industry. To achieve this, it was
302 necessary to define the physical meaning of the WRC parameter. The results of WRC
303 measurements are shown in Figure 8. The WRC values increased with the increasing MW
304 power. They were significantly ($p < 0.05$) higher for samples treated using HAD + 4 W/g
305 and HAD + 6 W/g than for HAD and HAD + 2 W/g treatments.

306 Considering the properties described above, it is possible to describe the sample
307 rehydration process by giving a physical meaning to the WRC. The hygroscopicity of the
308 sample will depend on the energy needed to adsorb water molecules and the swelling
309 capacity of the sample in its rubbery state. Figure 9 shows the isosteric heat of dried
310 samples against the WRC, for each drying treatment. The figure demonstrates that the
311 isosteric heat and the WRC increase with the increasing MW power. The isosteric heat is
312 directly related to the WRC; a rise in the energy of adsorption increases the value of
313 WRC.

314 To confirm the theory of shrinkage/swelling illustrated, at a macroscopic level, in Figure
315 7, it is necessary to analyse the microscopic deformations. Therefore, the photographs of
316 fresh and dried samples obtained using a stereomicroscope and Cryo-SEM techniques
317 were studied. Figure 10 shows fresh samples (Figure 10A), samples dehydrated by HAD
318 (Figure 10B) and by HAD + MW at three levels of MW power (after 60 min of drying; 2

W/g in Figure 10C, 4 W/g in 10D and 6 W/g in Figure 10E). One can see the peel tissue or flavedo (F) with the epidermal and hypodermal layers that surround a massive parenchyma or albedo (A) with numerous oil gland cavities or trichomes (T). The micrographs of fresh samples show spherical turgid cells, and spherical trichomes are visible in stereographic images (Figure 10A). The HAD samples display a general shrinkage of the tissue and are compacted (low gas phase). The trichomes shrank because of the peel contraction induced by the parenchymatic dehydration (Figure 10B). The micrographs in Figure 10 were obtained after 60 min of drying. At this time point, the samples undergoing the HAD + MW treatment showed macroscopic swelling, reflected in the volume variation plots (Figure 7). This phenomenon was also observed in the micrographs, which showed more gas phase in the HAD + MW specimens than in the HAD samples (Figure 10 C, D and E). The trichomes were deformed (this was also seen in samples treated using HAD) as a result of parenchymatic dehydration. However, these trichomes kept its overall volume because they contain mostly the essential oils (hydrophobic). Macroscopic swelling, shown in Figure 7 and Figure 10, was not evenly distributed; it was most intense in the parenchymatic tissue (albedo). This phenomenon is easier to see in Figure 11. As mentioned before, at the beginning of drying, the samples underwent a drastic reduction in volume associated with the evaporation of water from the surface. This caused shrinkage of the flavedo and produced a crusting effect on reaching the glass transition. The strong shrinkage of the flavedo and a weak contraction of the trichomes resulted in spherical, trichome-shaped bulges at the surface of the peel (Figure 11C). Furthermore, the internal evaporation induced by the microwaves produced swelling of the albedo, with a crisping effect at the point of glass transition. This increased the area available for water adsorption, thus increasing the WRC. Talens et al. 2017

showed that, during HAD + MW drying of orange by-products, an increase in porosity caused an increase in particle size, which improved fibre swelling capacity.

4. CONCLUSIONS

The desorption isotherms of orange peel dried using different treatments (HAD + MW) were obtained and analysed. The results showed that the GAB model could be used to predict the moisture levels using the a_w measurements. Thus, this model might become a useful tool for monitoring the dehydration process of orange peel. The macrostructural and microstructural transformations were demonstrated and discussed, taking into account the interactions of water with the tissue. The observed shrinkage/swelling phenomena clearly depended on the MW power and on the nature of the tissue. Therefore, it can be concluded that combining the microwave treatment and HAD not only reduces the processing time; it also generates microstructural changes in the dried tissue that increase its WRC. This improves the technological properties of this stabilised by-product, which will be of benefit during its further conversion into the dietary fibre.

5. ACKNOWLEDGEMENTS

The authors would like to thank the Basque Government for the financial support of the project (LasaiFood). They also acknowledge the financial support from the Spanish Ministerio de Economía, Industria y Competitividad, Programa Estatal de I+D+i orientada a los Retos de la Sociedad AGL2016-80643-R. This paper is contribution nº 777 from AZTI (Food Research Division). The authors would like to thank the Electronic Microscopy Service of the Universidad Politécnica de Valencia for its assistance in the use of Cryo-SEM.

6. REFERENCES

Al-Muhtaseb, A. H., McMinn, W. A. M., & Magee, T. R. A. (2002). Moisture Sorption Isotherm Characteristics of Food Products: A Review. *Food and Bioproducts Processing, 80*(2), 118-128, doi:http://dx.doi.org/10.1205/09603080252938753.

Andrade, R. D., Lemus, R., & Pérez, C. E. (2011). Models of sorption isotherms for food: uses and limitations. *Vitae, 18*(3), 325-334.

Bejar, A. K., Ghanem, N., Mihoubi, D., Kechaou, N., & Mihoubi, N. B. (2011). Effect of Infrared Drying on Drying Kinetics, Color, Total Phenols and Water and Oil Holding Capacities of Orange (Citrus Sinensis) Peel and Leaves. *International Journal of Food Engineering, 7*(5), doi:10.2202/1556-3758.2222.

Bergese, P. (2006). Specific heat, polarization and heat conduction in microwave heating systems: A nonequilibrium thermodynamic point of view. *Acta Materialia, 54*(7), 1843-1849, doi:10.1016/j.actamat.2005.11.042.

Castro-Giráldez, M., Fito, P. J., Chenoll, C., & Fito, P. (2010). Development of a dielectric spectroscopy technique for the determination of apple (Granny Smith) maturity. *Innovative Food Science & Emerging Technologies, 11*(4), 749-754, doi:http://dx.doi.org/10.1016/j.ifset.2010.08.002.

Castro-Giráldez, M., Fito, P. J., Dalla Rosa, M., & Fito, P. (2011a). Application of microwaves dielectric spectroscopy for controlling osmotic dehydration of kiwifruit (Actinidia deliciosa cv Hayward). *Innovative Food Science & Emerging Technologies, 12*(4), 623-627, doi:http://dx.doi.org/10.1016/j.ifset.2011.06.013.

Castro-Giráldez, M., Fito, P. J., & Fito, P. (2011b). Application of microwaves dielectric spectroscopy for controlling long time osmotic dehydration of parenchymatic apple tissue. *Journal of Food Engineering, 104*(2), 227-233, doi:http://dx.doi.org/10.1016/j.jfoodeng.2010.10.034.

Demirel, Y., & Sandler, S. I. (2001). Linear-nonequilibrium thermodynamics theory for coupled heat and mass transport. *International Journal of Heat and Mass Transfer, 44*(13), 2439-2451, doi:http://dx.doi.org/10.1016/S0017-9310(00)00291-X.

Edrisi Sormoli, M., & Langrish, T. A. G. (2015). Moisture sorption isotherms and net isosteric heat of sorption for spray-dried pure orange juice powder. *LWT - Food Science and Technology, 62*(1, Part 2), 875-882, doi:http://dx.doi.org/10.1016/j.lwt.2014.09.064.

Fava, F., Zanaroli, G., Vannini, L., Guerzoni, E., Bordoni, A., Viaggi, D., et al. (2013). New advances in the integrated management of food processing by-products in Europe: sustainable exploitation of fruit and cereal processing by-products with the production of new food products (NAMASTE EU). *New Biotechnology, 30*(6), 647-655, doi:http://dx.doi.org/10.1016/j.nbt.2013.05.001.

Fernández-López, J., Sendra-Nadal, E., Navarro, C., Sayas, E., Viuda-Martos, M., & Alvarez, J. A. P. (2009). Storage stability of a high dietary fibre powder from orange by-products. *International Journal of Food Science & Technology, 44*(4), 748-756, doi:10.1111/j.1365-2621.2008.01892.x.

Ghanem, N., Mihoubi, D., Kechaou, N., & Mihoubi, N. B. (2012). Microwave dehydration of three citrus peel cultivars: Effect on water and oil retention capacities, color, shrinkage and total phenols content. *Industrial Crops and Products, 40*(0), 167-177, doi:http://dx.doi.org/10.1016/j.indcrop.2012.03.009.

Gómez, A., López, R., Esturo, A., Bald, C., Tueros, I., Talens, C., & Raynaud, C. (2015). From waste products to raw materials for the development of new foods. *Proceedings of the Institution of Civil Engineers - Waste and Resource Management*, 168(2), 55-62. doi: doi:10.1680/warm.13.00038

Hossain, M. D., Bala, B. K., Hossain, M. A., & Mondol, M. R. A. (2001). Sorption isotherms and heat of sorption of pineapple. [Article]. *Journal of Food Engineering, 48*(2), 103-107, doi:10.1016/s0260-8774(00)00132-1.

Igual, M., Contreras, C., & Martinez-Navarrete, N. (2010). Non-conventional techniques to obtain grapefruit jam. *Innovative Food Science & Emerging Technologies, 11*(2), 335-341.

Kowalski, S. J., Rajewska, K., & Rybicki, A. (2005). Stresses generated during convective and microwave drying. *Drying Technology, 23*(9-11), 1875-1893, doi:10.1080/07373930500210226.

Labuza, T. P., Altunakar, B. (2007). Water Activity Prediction and Moisture Sorption Isotherms. In G. V. Barbosa-Cánovas, A. J. Fontana, S. J. Schmidt, & T. P. Labuza (Eds.), *Water Activity in Foods: Fundamentals and Applications* (Vol. 109-154). Iowa, USA: IFT Press and Blackwell Publishing.

Larrauri, J. A. (1999). New approaches in the preparation of high dietary fibre powders from fruit by-products. *Trends in Food Science & Technology, 10*(1), 3-8.

Martín, M. E., Martínez-Navarrete, N., Chiralt, A., Fito, P. (2003). Diseño y construcción de una instalación experimental para el estudio de la cinética de secado combinado por aire caliente y microondas. *Alimentación equipos y tecnología, 22*(181), 101-107.

Quirijns, E. J., van Boxtel, A. J. B., van Loon, W. K. P., & van Straten, G. (2005). Sorption isotherms, GAB parameters and isosteric heat of sorption. *Journal of the Science of Food and Agriculture, 85*(11), 1805-1814, doi:10.1002/jsfa.2140.

Rizvi, S. S. H., & Benado, A. L. (1984). Thermodynamic properties of dehydrated foods. *Food Technology, 38*(3), 83-92.

441 Robertson, J. A., de Monredon, F. D., Dysseler, P., Guillon, F., Amado, R., & Thibault,
442 J.-F. (2000). Hydration Properties of Dietary Fibre and Resistant Starch: a
443 European Collaborative Study. [doi: DOI: 10.1006/fstl.1999.0595]. *Lebensmittel-*
444 *Wissenschaft und-Technologie, 33*(2), 72-79.
445 Schieber, A., Stintzing, F. C., & Carle, R. (2001). By-products of plant food processing
446 as a source of functional compounds - recent developments. *Trends in Food*
447 *Science & Technology, 12*(11), 401-+.
448 Schiffmann, R. (2001). Microwave processes for the food industry. In Datta, A. &
449 Anantheswaran, R. (Ed.), *Handbook of Microwave Technology for Food*
450 *Applications* (pp. 299–352). New York: Marcel Dekker.
451 Talens, C., Castro-Giráldez, M., & Fito, P. J. (2016a). A thermodynamic model for hot-
452 air microwave drying of orange peel. *Journal of Food Engineering, 175, 33-42,*
453 *http://dx.doi.org/10.1016/j.jfoodeng.2015.12.001*
454 Talens, C., Castro-Giráldez, M., & Fito, P. J. (2016b). Study of the effect of microwave
455 power coupled with hot air drying on orange peel by dielectric spectroscopy. *LWT*
456 *- Food Science and Technology*, 66, 622-628,
457 http://dx.doi.org/10.1016/j.lwt.2015.11.015.
458 Talens, C., Arboleya, J. C., Castro-Giraldez, M., & Fito, P. J. (2017). Effect of microwave
459 power coupled with hot air drying on process efficiency and physico-
460 chemical properties of a new dietary fibre ingredient obtained from orange
461 peel. *LWT - Food Science and Technology*, 77, 110-118,
462 doi:http://doi.org/10.1016/j.lwt.2016.11.036.
463 Traffano-Schiffo, M. V., Castro-Giráldez, M., Fito, P. J., & Balaguer, N. (2014).
464 Thermodynamic model of meat drying by infrarred thermography. *Journal of*

Food Engineering, *128*(0), 103-110, doi:http://dx.doi.org/10.1016/j.jfoodeng.2013.12.024.

Traffano-Schiffo, M. V., Castro-Giráldez, M., Colom, R.J. & Fito, P. J. (2015). Study of the application of dielectric spectroscopy to predict the water activity of meat during drying process. *Journal of Food Engineering*, 166, 285–290, http://dx.doi.org/10.1016/j.jfoodeng.2015.06.030

van den Berg, C., Bruin, S. (1981). Water activity and its estimation in food systems—theoretical aspects. In L. B. R. a. G. F. Stewart (Ed.), *Water Activity: Influences on Food Quality* (pp. 1–61). New York, NY, USA: Academic Press.

Waldron, K. W. (2009). Part III Exploitation of co-products as food and feed ingredients. In Waldron, K. W. (Ed.). *Handbook of Waste Management and Co-Product Recovery in Food Processing* (pp.255-265). U.K.,: Elsevier Science.

Yan, Z., Sousa-Gallagher, M. J., & Oliveira, F. A. R. (2008). Sorption isotherms and moisture sorption hysteresis of intermediate moisture content banana. *Journal of Food Engineering*, *86*(3), 342-348, doi:10.1016/j.jfoodeng.2007.10.009.

483 FIGURE CAPTIONS

484 Figure 1. Schematic diagram of the experimental procedure.

485 Figure 2. Schematic description of the laboratory equipment used to dry the samples.

486 Figure 3. Drying curves for orange peel during different treatments: ●, HAD; ◆, HAD
487 + 2 W/g; ▲, HAD + 4 W/g and ●, HAD + 6 W/g. Data represent means and standard
488 deviations of experiments performed in triplicate.

489 Figure 4. Sorption isotherms for orange peel dried using different treatments.
490 Experimental points: ●, HAD; ◆, HAD + 2 W/g; ▲, HAD + 4 W/g and ●, HAD + 6
491 W/g. GAB model: –, HAD; –, HAD + 2 W/g; - - -, HAD + 4 W/g and - · -, HAD + 6 W/g.

492 Figure 5. GAB model parameters. ▲, monomolecular moisture layer X_{W0}. ■, energy
493 constant (C) for isotherms of orange peel dried using different hot air–microwave
494 treatments.

495 Figure 6. Sorption isosteric heat versus the moisture of orange peel samples treated by
496 MW at different power: ●, HAD; ◆, HAD + 2 W/g; ▲, HAD + 4 W/g and ●, HAD + 6
497 W/g. The inset shows the Q_c values of dried product for the different MW power
498 treatments.

499 Figure 7. Volume variation of orange peel dried using different treatments: ●, HAD; ◆,
500 HAD + 2 W/g; ▲, HAD + 4 W/g and ●, HAD + 6 W/g. Data represent means and standard
501 deviations of experiments performed in triplicate.

502 Figure 8. Water retention capacity (kg_w/kg_{dm}) of orange peel dried using different
503 treatments: ●, HAD; ◆, HAD + 2 W/g; ▲, HAD + 4 W/g and ●, HAD + 6 W/g. Data
504 represent means and standard deviations of experiments performed in triplicate.

505 Figure 9. Isosteric heat of dried product versus its water retention capacity

Figure 10. Micrographs of fresh and dried orange peel samples (60 min of drying). (A), fresh orange peel samples, 1000×; (B), HAD samples, 1000×; (C), HAD + 2 W/g, 1000×; (D), HAD + 4 W/g, 200× and (E), HAD + 6 W/g, 200×. F, Flavedo; A, Albedo; T, Trichomes.

Figure 11. Micrographs of orange peel samples (A) dried using HAD + 2 W/g for 60 min, (B) HAD + 6 W/g for 60 min and (C) HAD + 6 W/g for 120 min. F, Flavedo; A, Albedo; T, Trichomes.

FIGURE CAPTIONS

Figure 1. Schematic diagram of the experimental procedure.

Figure 2. Schematic description of the laboratory equipment used to dry the samples.

Figure 3. Drying curves for orange peel during different treatments: ●, HAD; ◆, HAD + 2 W/g; ▲, HAD + 4 W/g and ●, HAD + 6 W/g. Data represent means and standard deviations of experiments performed in triplicate.

Figure 4. Sorption isotherms for orange peel dried using different treatments. Experimental points: ●, HAD; ◆, HAD + 2 W/g; ▲, HAD + 4 W/g and ●, HAD + 6 W/g. GAB model: –, HAD; –, HAD + 2 W/g; - - -, HAD + 4 W/g and - · -, HAD + 6 W/g.

Figure 5. GAB model parameters. ▲, monomolecular moisture layer X_{W0}. ■, energy constant (C) for isotherms of orange peel dried using different hot air–microwave treatments.

Figure 6. Sorption isosteric heat versus the moisture of orange peel samples treated by MW at different power: ●, HAD; ◆, HAD + 2 W/g; ▲, HAD + 4 W/g and ●, HAD + 6 W/g. The inset shows the Q_c values of dried product for the different MW power treatments.

Figure 7. Volume variation of orange peel dried using different treatments: ●, HAD; ◆, HAD + 2 W/g; ▲, HAD + 4 W/g and ●, HAD + 6 W/g. Data represent means and standard deviations of experiments performed in triplicate.

Figure 8. Water retention capacity (kg_w/kg_{dm}) of orange peel dried using different treatments: ●, HAD; ◆, HAD + 2 W/g; ▲, HAD + 4 W/g and ●, HAD + 6 W/g. Data represent means and standard deviations of experiments performed in triplicate.

Figure 9. Isosteric heat of dried product versus its water retention capacity

Figure 10. Micrographs of fresh and dried orange peel samples (60 min of drying). (A), fresh orange peel samples, 1000×; (B), HAD samples, 1000×; (C), HAD + 2 W/g, 1000×; (D), HAD + 4 W/g, 200× and (E), HAD + 6 W/g, 200×. F, Flavedo; A, Albedo; T, Trichomes.

Figure 11. Micrographs of orange peel samples (A) dried using HAD + 2 W/g for 60 min, (B) HAD + 6 W/g for 60 min and (C) HAD + 6 W/g for 120 min. F, Flavedo; A, Albedo; T, Trichomes.

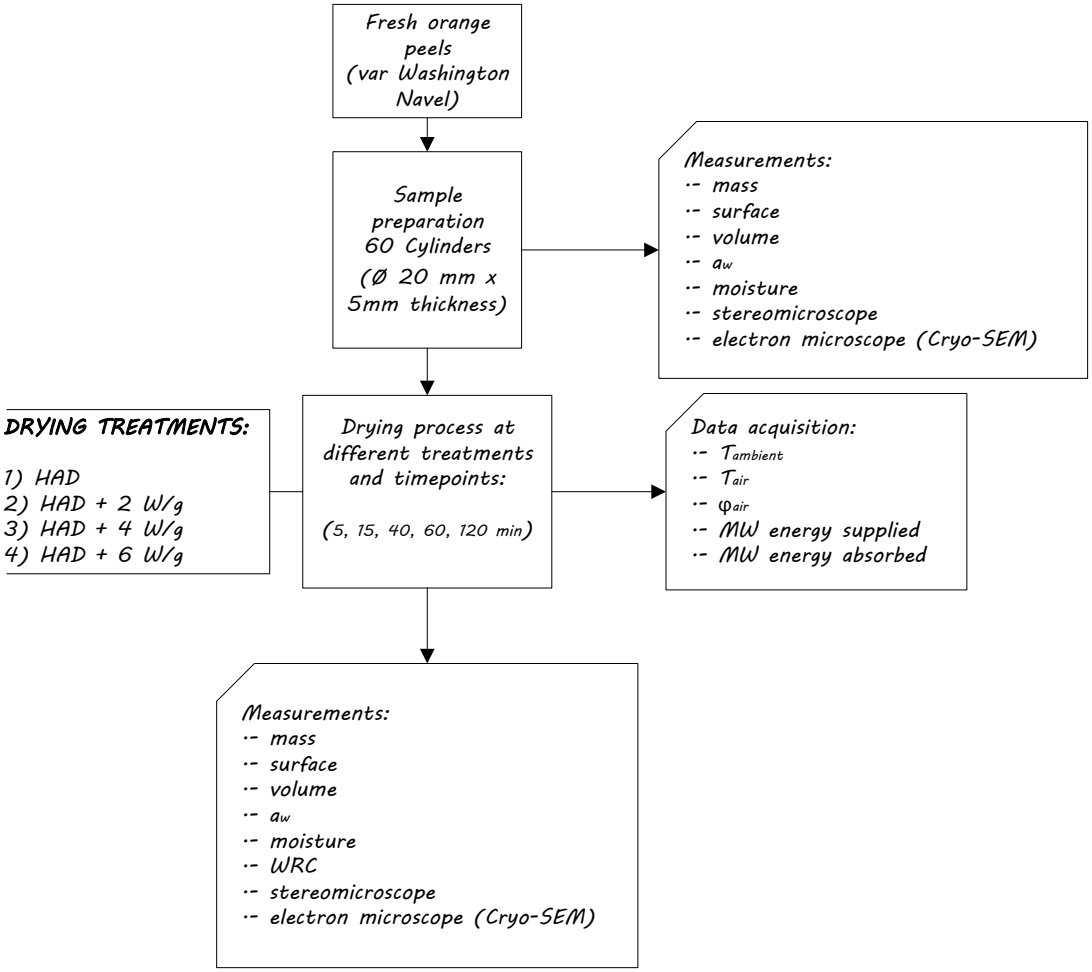
Fresh orange peels (var Washington Navel)
Sample preparation 60 Cylinders (Ø 20 mm x 5mm thickness)
Measurements:
·- mass
·- surface
·- volume
·- aw
·- moisture
·- stereomicroscope
·- electron microscope (Cryo-SEM)
DRYING TREATMENTS:
1) HAD
2) HAD + 2 W/g
3) HAD + 4 W/g
4) HAD + 6 W/g
Drying process at different treatments and timepoints:
(5, 15, 40, 60, 120 min)
Data acquisition:
·- Tambient
·- Tair
·- φair
·- MW energy supplied
·- MW energy absorbed
Measurements:
·- mass
·- surface
·- volume
·- aw
·- moisture
·- WRC
·- stereomicroscope
·- electron microscope (Cryo-SEM)

Figure 1

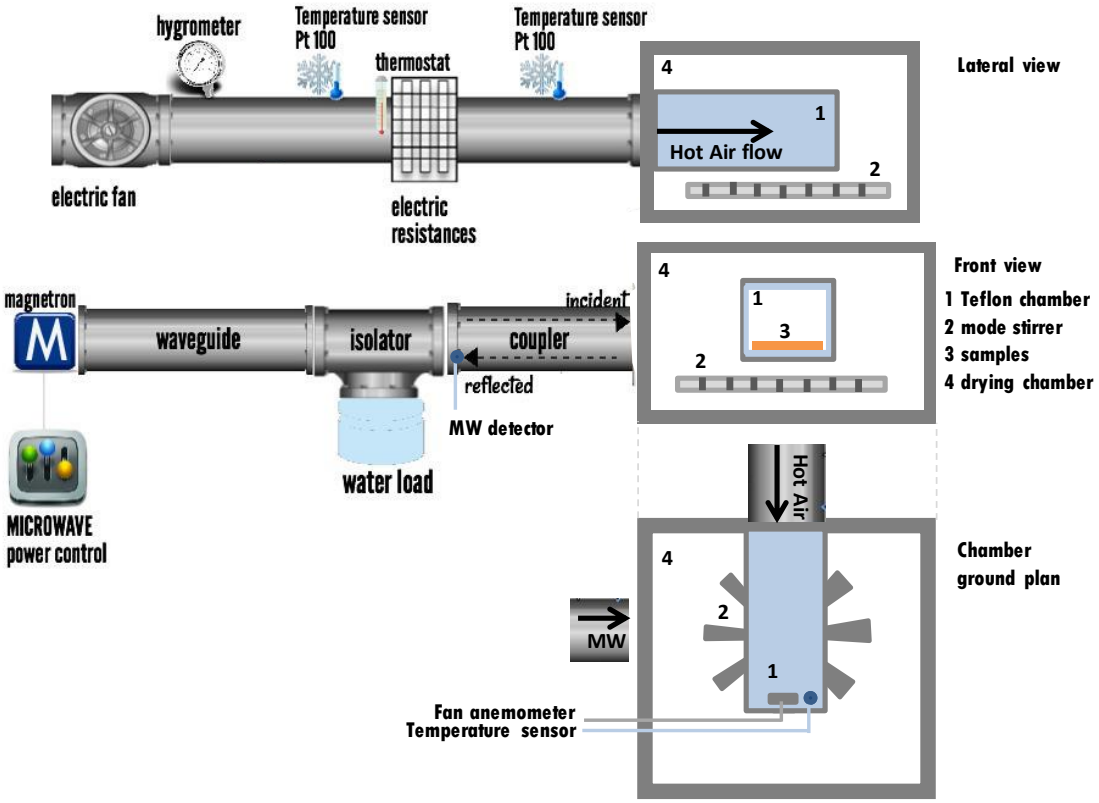
hygrometer
Temperature sensor Pt 100
thermostat
Temperature sensor Pt 100
electric fan
electric resistances
4
1
Hot Air flow
2
Lateral view
magnetron
M
waveguide
isolator
coupler
incident
reflected
MW detector
water load
MICROWAVE power control
4
1
3
2
Front view
1 Teflon chamber
2 mode stirrer
3 samples
4 drying chamber
Hot Air
4
2
1
MW
Fan anemometer
Temperature sensor
Chamber ground plan

Figure 2.

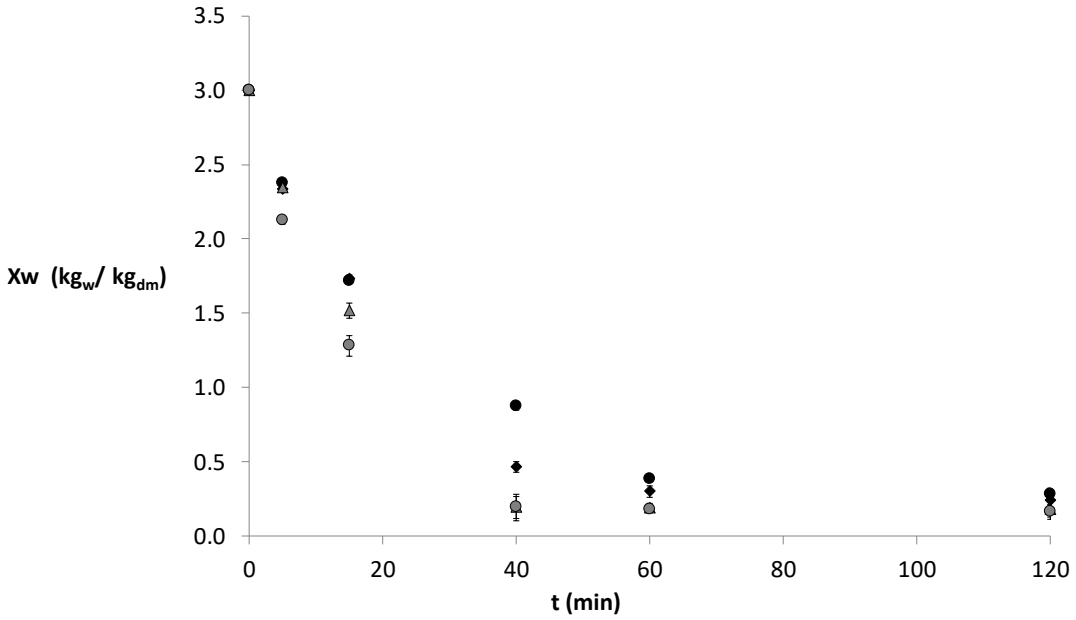

Figure 3.

Figure 4 Click here to download Figure Figure 4.pdf

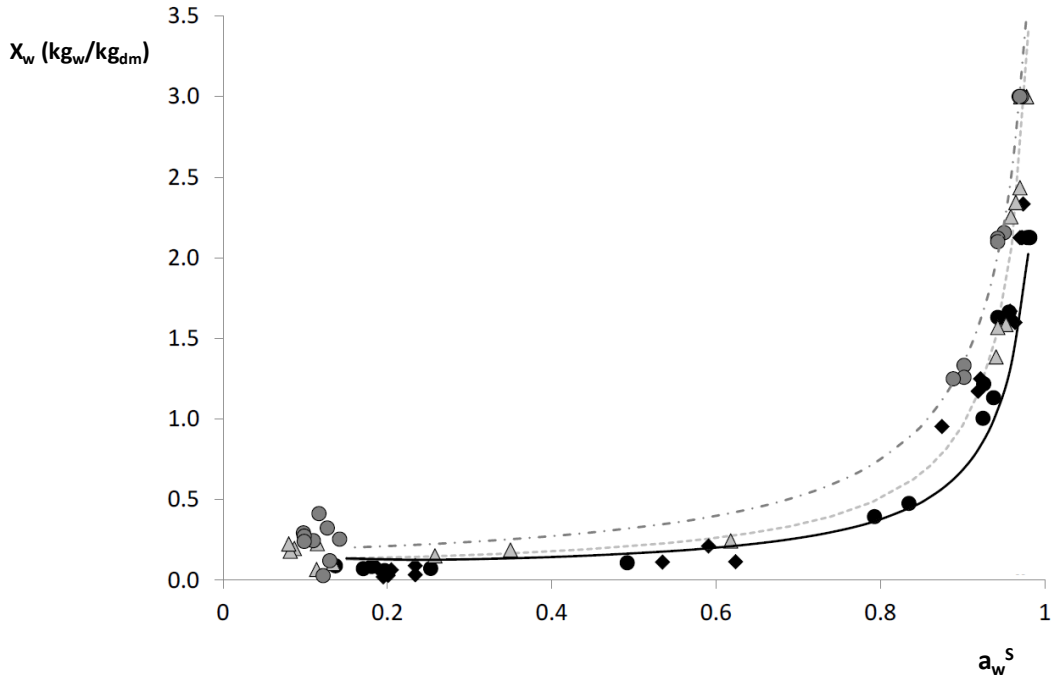

Figure 4

Figure 5 Click here to download Figure Figure 5.pdf

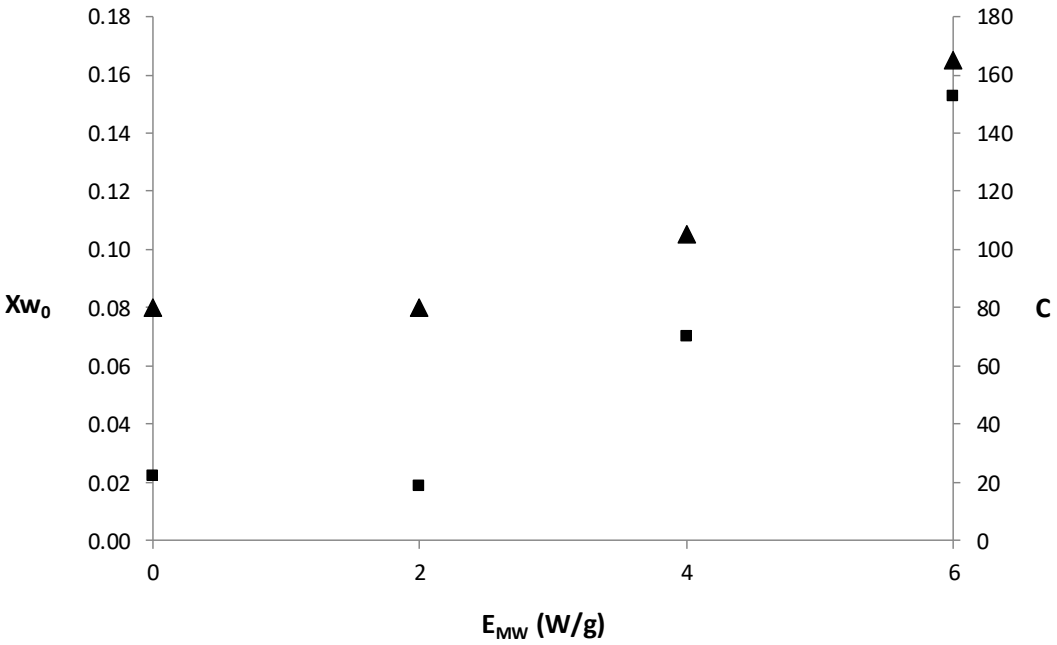

Figure 5.

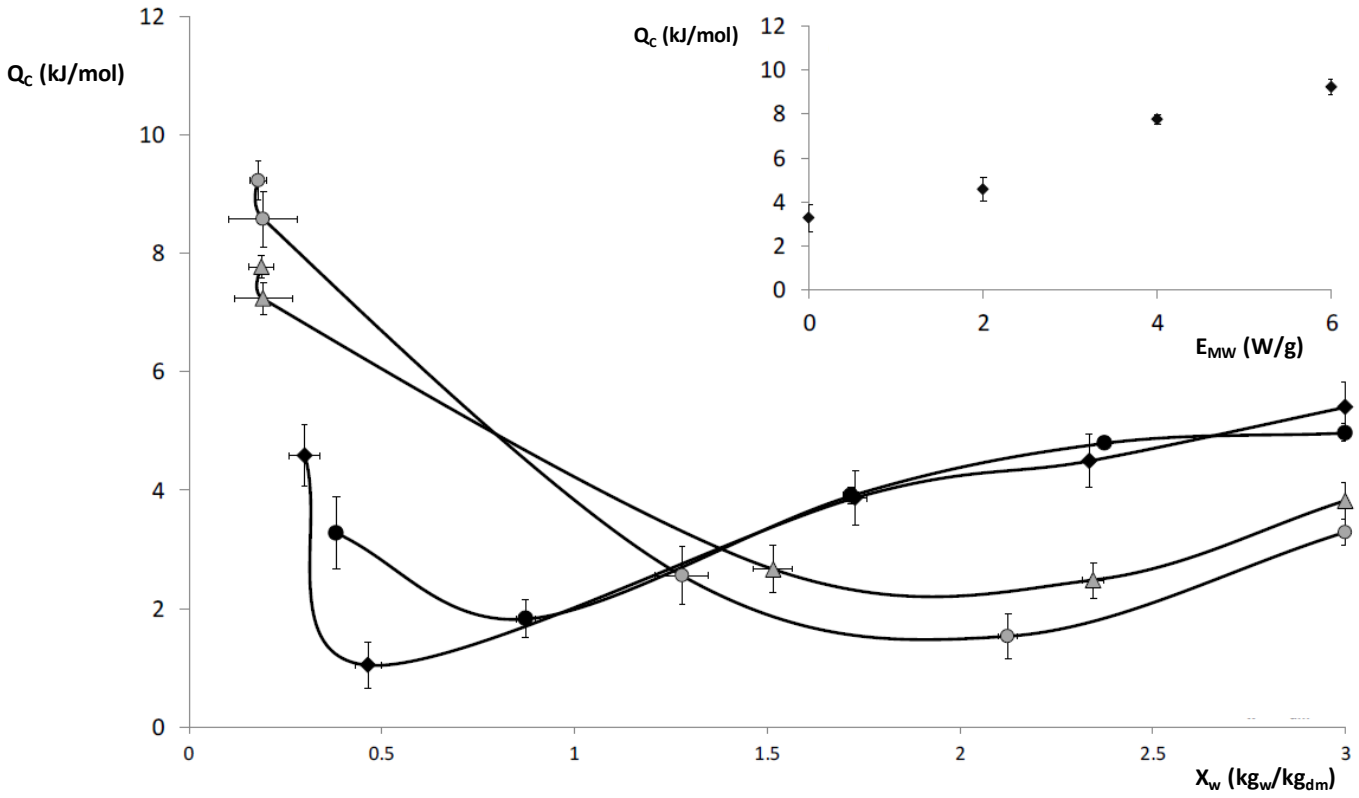

Figure 6

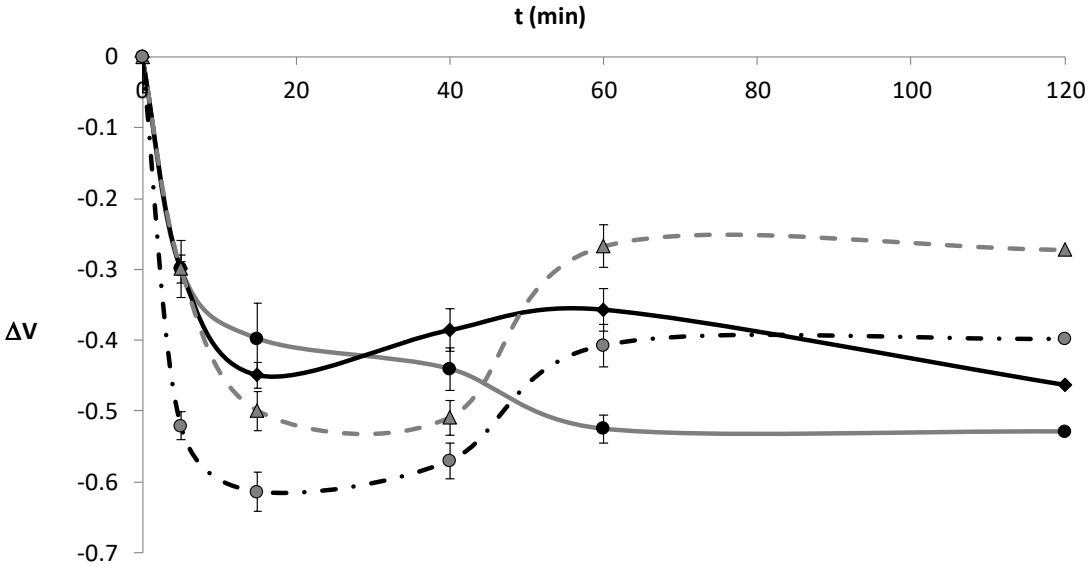

Figure 7.

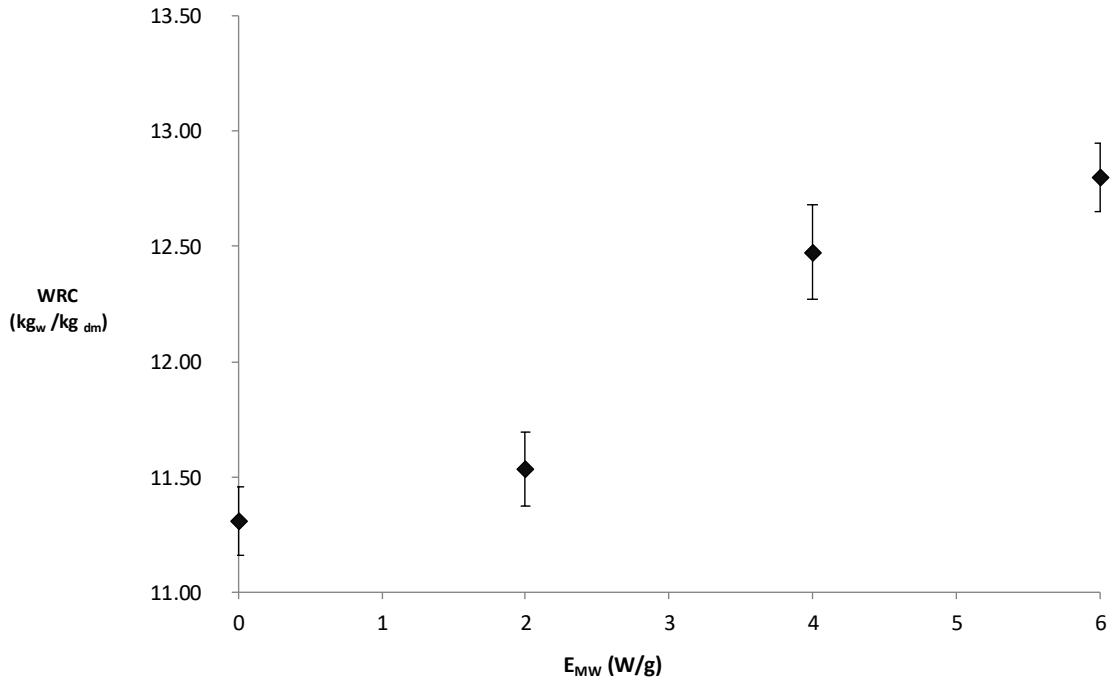

Figure 8.

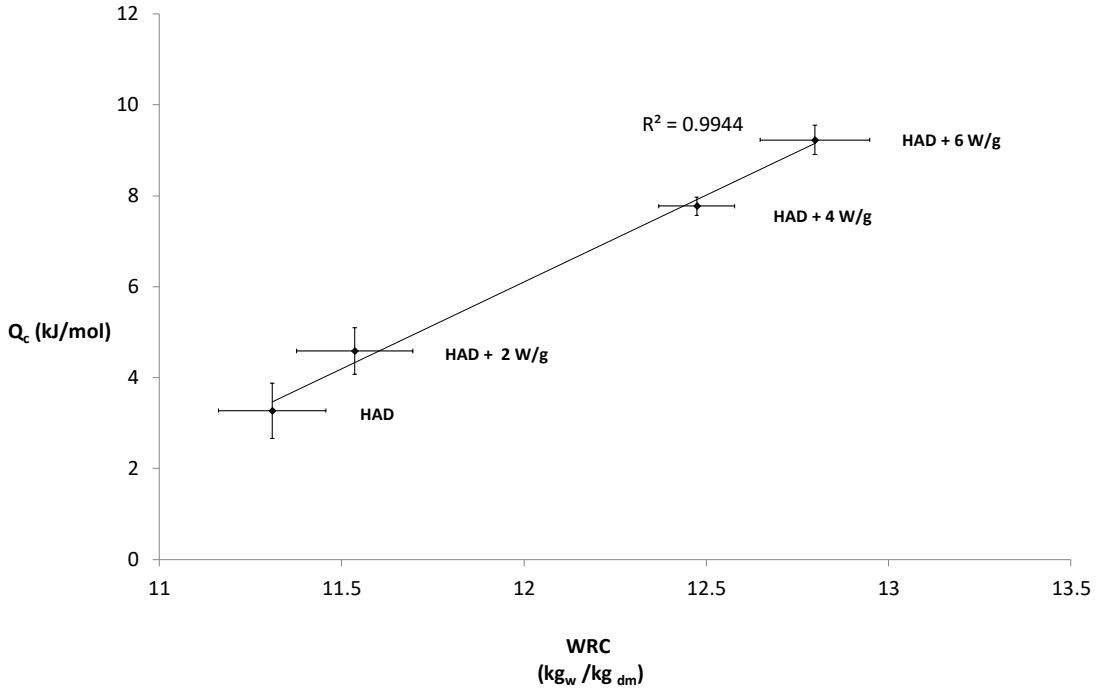

Figure 9.

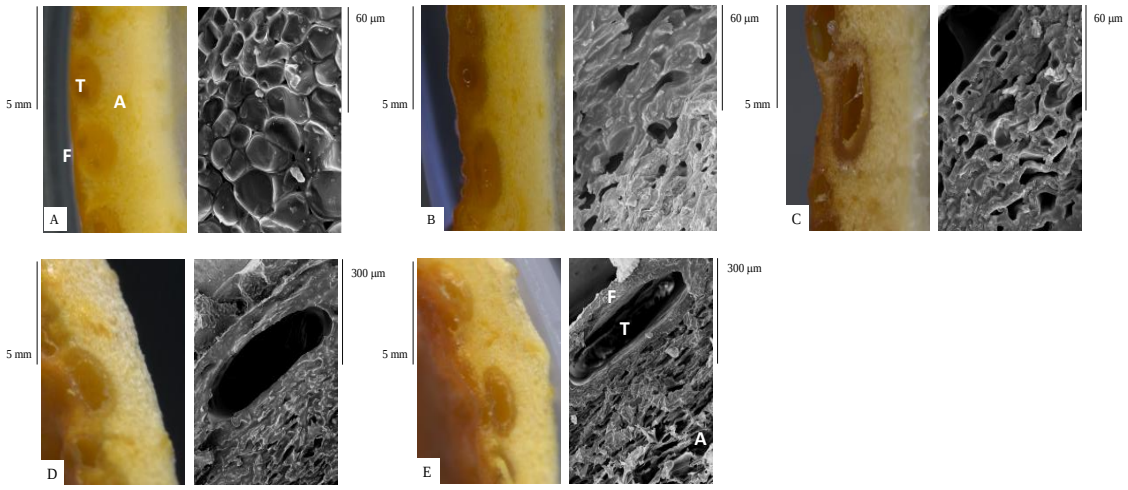

Figure 10.

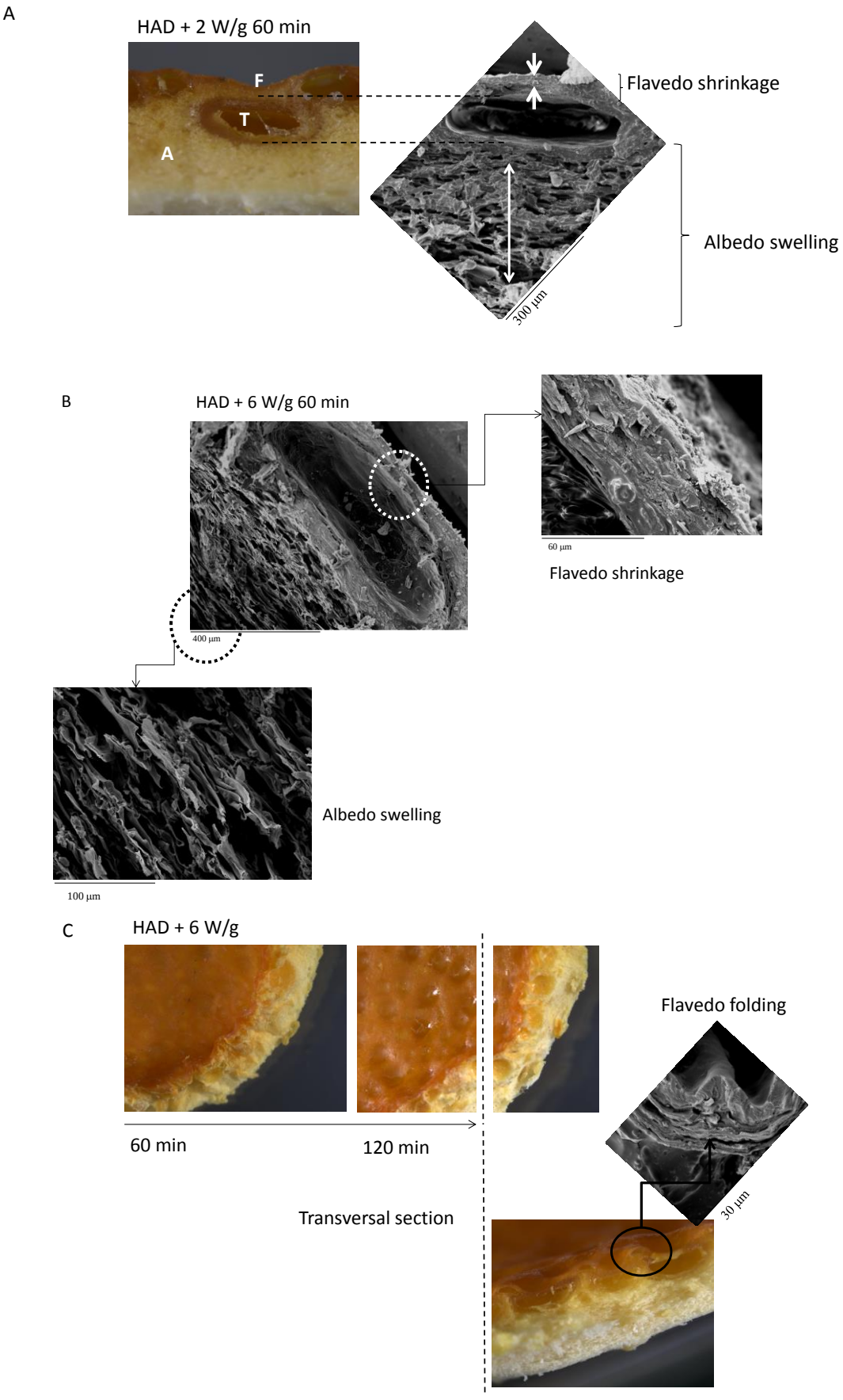

Figure 11.